

Let. 31, 301 (1973).

<sup>8</sup>Y. Yafet, Phys. Rev. 115, 1172 (1959); R. Bowers and Y. Yafet, Phys. Rev. 115, 1165 (1959).

<sup>9</sup>W. Zawadzki, in *New Developments in Semiconductors*, edited by P. R. Wallace (Nordhoff, Gronigen, The Netherlands, 1973), p. 441; P. Kacman and W. Zawadzki, Phys. Status Solidi (b) 47, 629 (1971).

<sup>10</sup>S. T. Pavlov and Yu. A. Firsov, Fiz. Tverd. Tela 7, 2634 (1965), and 9, 1780 (1967) [Sov. Phys. Solid State 7, 2131 (1965), and 9, 1394 (1967)], and Zh. Eksp. Teor. Fiz. 49, 1664 (1965) [Sov. Phys. JETP 22, 1137 (1966)], considered spin-phonon interaction using a complicated procedure based on the Luttinger-Kohn transformation. Both our approach and final results for polar and nonpolar coupling differ from theirs.

<sup>11</sup>G. L. Bir and G. E. Pikus, Fiz. Tverd. Tela 2, 2287

(1960) [Sov. Phys. Solid State 2, 2039 (1960)].

<sup>12</sup>K. L. Ngai, private communication. Our value of  $d_0$  is  $\sqrt{\frac{3}{2}}$  times smaller than the one usually defined.

<sup>13</sup>J. R. Barker and B. Magnusson, in *Proceedings of the Twelfth International Conference on the Physics of Semiconductors, Stuttgart, Germany, 1974*, edited by M. H. Pilkuhn (Teubner, Stuttgart, 1974,) p. 811.

<sup>14</sup>W. Zawadzki, to be published.

<sup>15</sup>R. A. Stradling and R. A. Wood, J. Phys. C: Solid State Phys. 3, 2425 (1970).

<sup>16</sup>G. Bauer, E. Erkinger, H. Kahlert, and W. Racek, J. Phys. E: Sci. Instrum. 6, 186 (1973); W. Racek, to be published.

<sup>17</sup>Kh. I. Amirkhanov, R. I. Bashirov, and V. A. Elizarov, Fiz. Tverd. Tela 17, 361 (1975) [Sov. Phys. Solid State 17, 230 (1975)].

## Temperature-Dependent Susceptibility of the Symmetric Anderson Model: Connection to the Kondo Model

H. R. Krishna-murthy,\* K. G. Wilson,† and J. W. Wilkins‡  
*Department of Physics, Cornell University, Ithaca, New York 14853*  
 (Received 11 August 1975)

The temperature-dependent impurity susceptibility for the symmetric Anderson Hamiltonian is discussed for all physically relevant values of its parameters  $U$  (the Coulomb correlation energy) and  $\Gamma$  (the  $d$ -level width). For  $U > \pi\Gamma$ , the results, for temperatures less than  $U/10k_B$ , map onto those of the spin- $\frac{1}{2}$  Kondo Hamiltonian with an effective exchange constant given by  $\rho J_{\text{eff}} = -8\Gamma/\pi U$ . At higher temperatures the results show the formation of the local moment from the free orbital.

We report here the results of the first calculation of the temperature-dependent impurity susceptibility for a magnetic impurity in a nonmagnetic metal describable by the symmetric Anderson model<sup>1</sup> over the full, physically relevant range of the parameters of that model. The calculation is based on the numerical renormalization-group techniques developed by Wilson for the spin- $\frac{1}{2}$  Kondo Hamiltonian.<sup>2,3</sup> The results are expected to be accurate to a few percent.

Among the noteworthy features of the results are the following: (1) Within certain ranges of the parameters there exists a temperature region where the model has a local moment, as indicated by a Curie-Weiss susceptibility. (2) At low enough temperatures this moment is always compensated by the conduction electrons and the impurity susceptibility approaches a constant at zero temperature. (3) The low-temperature susceptibility maps precisely onto that of the spin- $\frac{1}{2}$  Kondo Hamiltonian.

The Hamiltonian for the symmetric Anderson

model is<sup>1</sup>

$$H_A = \sum_{ks} \epsilon_k n_{ks} - \frac{1}{2} U \sum_s n_{ds} + U n_{d\uparrow} n_{d\downarrow} + V \sum_{ks} (c_{ds}^\dagger c_{ks} + c_{ks}^\dagger c_{ds}). \quad (1)$$

We assume that the conduction electrons (whose energies are measured relative to the Fermi level) are in an isotropic band of constant density of states per spin  $\rho$  within a bandwidth  $2D$ . The symmetry<sup>4</sup> of the Hamiltonian is that while the first electron in the localized  $d$  orbital has energy  $-U/2$ , because of the Coulomb repulsion energy  $U$ , a second electron in the orbital has energy  $+U/2$ . The coupling  $V$  between the localized  $d$  orbital and the conduction band leads to a  $d$ -level width<sup>1</sup>

$$\Gamma = \pi \rho V^2. \quad (2)$$

When  $\Gamma \ll U$  one expects<sup>1,5</sup> the model to display a local moment and to be describable by a spin- $\frac{1}{2}$  Kondo Hamiltonian

$$H_K = \sum_{ks} \epsilon_k n_{ks} - \mathcal{J} \vec{S}(0) \cdot \vec{S}_d, \quad (3)$$

where  $\tilde{S}_d$  is the impurity spin and  $\tilde{s}(0)$  the conduction electron spin density at the impurity site. Perturbation theory in  $\Gamma/U$  leads to a value of the exchange coupling constant  $J$ , given by<sup>5</sup>

$$\rho J_{\text{eff}} = -8\Gamma/\pi U, \quad (4)$$

to lowest order. This result turns out to be relevant even when  $\rho|J_{\text{eff}}|$  is not small.

Because of the close connection between  $H_A$  and  $H_K$  we review briefly the results<sup>3,6</sup> for the impurity susceptibility for the Kondo Hamiltonian. The "universal" (i.e., independent of  $J$  and of band-edge effects) function  $\Phi(y)$  plays a central role and is plotted in Fig. 1 (along the upper abscissa with its argument given by the right-hand ordinate). The susceptibility for the spin- $\frac{1}{2}$  Kondo Hamiltonian for  $k_B T \ll D$ , also shown in Fig. 1, is given by the implicit equation

$$\Phi(4k_B T \chi(T)/(g\mu_B)^2 - 1) = \ln[T/T_K(J)]. \quad (5)$$

Here  $g\mu_B/\hbar$  is the gyromagnetic ratio. The essential point about (5) is that  $\chi$  depends on  $J$  and on band-edge effects only through the Kondo temperature  $T_K(J)$ , given by

$$k_B T_K(J) = \tilde{D}(J) \exp[-\Phi(\rho J)], \quad (6)$$

where  $\tilde{D}(J)$  is an effective band edge of order  $D$  with a *regular* (but nonuniversal) power series expansion in  $\rho J$ . The argument of the exponential in (6) is the same universal function as in (5), which for  $|y| \ll 1$  is given by  $\Phi(y) = -y^{-1} - \frac{1}{2} \ln|y| + O(y)$ . Hence, for  $\rho|J| \ll 1$ , one recovers the by-

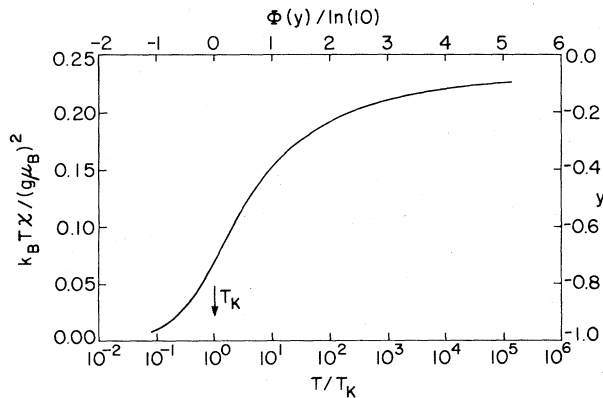


FIG. 1. Universal plot of  $k_B T \chi(T)/(g\mu_B)^2$  versus  $\ln(T/T_K)$ , where  $\chi(T)$  is the impurity susceptibility for the spin- $\frac{1}{2}$  Kondo Hamiltonian at low temperatures ( $k_B T \ll D$ ), and  $T_K$  is the Kondo temperature. The same plot also serves as a graph of the universal function  $\Phi(y)$  introduced in the text [cf. Eq. (5) and (6)].

now standard result<sup>3,7</sup> for the Kondo temperature,

$$T_K(J) = \tilde{D}(0) (\rho|J|)^{1/2} \exp(-1/\rho|J|), \quad (7)$$

$$\rho|J| \ll 1.$$

Several features of Fig. 1 should be noted. At high temperatures  $\chi(T)$  approaches the Curie result of  $\frac{1}{4}(g\mu_B)^2/k_B T$ . For  $T > T_K$ , over any decade of temperature  $\chi(T)$  is Curie-Weiss like with a decreased effective moment. For example, for  $T_K < T < 20T_K$ ,  $\chi \approx 0.17(g\mu_B)^2/k_B(T + 2T_K)$ . We refer to this region ( $T \gtrsim T_K$ ) as the *local-moment regime*. On the other hand, for  $T \ll T_K$  the local moment is compensated by the conduction electrons. In this *strong-coupling regime*,  $\chi(T)$  approaches the constant value  $0.1(g\mu_B)^2/k_B T_K$ . These two regimes will also appear in the results for the Anderson model.

Figure 2 shows susceptibility plots for the symmetric Anderson model for two different values of  $\Gamma/U$ . The rather small value of  $U/D = 10^{-3}$  has been chosen so as to spread out the various regimes that arise from the Anderson-model calculations. To guide the understanding of the plots in Fig. 2, we show in Fig. 3 a schematic depiction of these regimes. Note that the separation between the various regimes (to be discussed below) is quite fuzzy, there being no sharp transi-

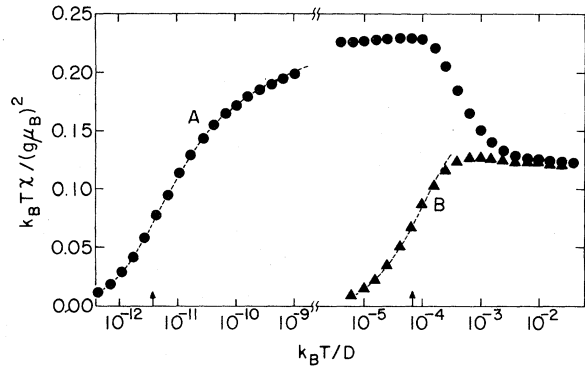


FIG. 2. Plots of  $k_B T \chi(T)/(g\mu_B)^2$  versus  $\ln(k_B T/D)$ , where  $\chi(T)$  is the impurity susceptibility for the symmetric Anderson model, for two different values of  $\Gamma/U$ . The value of  $U/D$  is  $10^{-3}$  for both plots. Plot A has a  $\Gamma$  value such that  $\rho J_{\text{eff}} = -8\Gamma/\pi U$  is  $-0.064$ , whereas plot B corresponds to  $\rho J_{\text{eff}} = -0.800$ . The dashed curves are obtained by sliding the universal curve of Fig. 1 over Fig. 2 so as to make it line up with the low-temperature ends of plots A and B. The vertical arrows mark the positions of  $T_K$  when the two figures are so aligned, and determine the values of the effective Kondo temperature  $T_K(\Gamma, U)$  [cf. Eq. (8)] for the two cases.

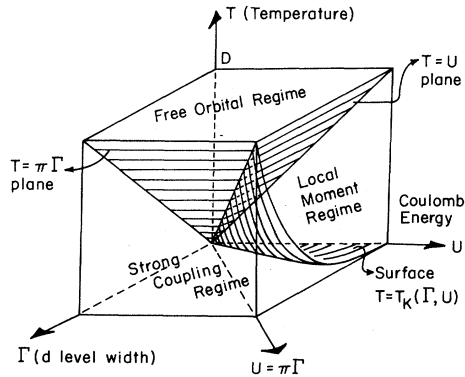


FIG. 3. Schematic sketch of the various regimes arising from the susceptibility results for the symmetric Anderson model. Note that the separations between the various regimes, in contrast to the drawing, are actually quite fuzzy.

tions in the Anderson (or Kondo) Hamiltonian.

Consider plot A in Fig. 2. The value of  $\Gamma$  for this plot corresponds, via (4), to  $\rho J_{\text{eff}} = -0.064$ . Hence this plot depicts  $\chi(T)$  along a vertical line in Fig. 3 lying close to the  $T$ - $U$  plane. For  $U < k_B T < D$  (possible since  $U/D = 10^{-3}$ ), the empty and the doubly occupied impurity states are nearly as likely to be populated as the singly occupied (with either spin) impurity state. Consequently in this regime the impurity susceptibility is close to that of a *free orbital*; i.e.,  $\chi(T) \approx \frac{1}{8} (g\mu_B)^2 / k_B T$ . As the temperature decreases below  $U$ ,  $k_B T \chi(T)$  increases, indicating the formation of the local moment (which is fully formed when  $k_B T \sim U/10$ ). For plot A, the *local-moment regime*, over which  $\chi(T)$  is Curie-Weiss like with a diminished effective moment, persists for six decades of temperature. (Note the break in the logarithmic temperature scale.) Finally at very low temperatures,  $k_B T \chi$  drops rapidly, approaching zero at zero temperature.

Plot B in Fig. 2 is for  $\rho J_{\text{eff}} = -0.800$ , corresponding to a vertical line in Fig. 3 lying close to the  $U = \pi\Gamma$  plane. In this case the *free-orbital regime* turns almost immediately into a region in which  $k_B T \chi(T)$  is strongly decreasing.

The common feature of plots A and B is that  $k_B T \chi(T)$  has a rapid decrease at low temperatures very similar to the result for the Kondo Hamiltonian in Fig. 1. In fact there is an extraordinary relation between Figs. 1 and 2. Since both figures have a logarithmic temperature scale, we may slide Fig. 1 horizontally on top of Fig. 2 to see if the universal curve of Fig. 1, obtained for

the Kondo Hamiltonian, lines up with the low-temperature ends of the susceptibility plots for the symmetric Anderson Hamiltonian. The dashed curves in Fig. 2 represent the results of such alignments. The agreement is perfect, within the accuracy of the computation. This is true not only for the two cases in Fig. 2 but for all that we have investigated, including cases when  $U \sim D$ . Finally note that the vertical arrows in Fig. 2 mark the points on its abscissa which coincide with the point  $T_K$  of Fig. 1 when the two figures are aligned as discussed above. These points hence determine effective Kondo temperatures for the Anderson Hamiltonian.

To summarize, the nature of the mapping of the symmetric Anderson Hamiltonian to the spin- $\frac{1}{2}$  Kondo Hamiltonian is that for  $\pi\Gamma < U$ , the low-temperature susceptibility for the Anderson Hamiltonian is also given by (5), but with a new scaling temperature  $T_K(\Gamma, U)$ . The numerical results that have been obtained for this effective Kondo temperature fit an expression of the form [compare (6)]

$$T_K(\Gamma, U) = \frac{1}{12} U [1 + f(\rho J_{\text{eff}})] \exp[-\Phi(\rho J_{\text{eff}})], \quad (8)$$

where  $f$  is a regular power-series expansion in  $\rho J_{\text{eff}}$  [ $f(0) = 0$ ]. Especially note that  $\rho J_{\text{eff}}$  is given by (4), i.e.,  $\rho J_{\text{eff}} = -8\Gamma/\pi U$ . That this result is relevant far beyond the range of its derivation is remarkable, but understandable in terms of the techniques used in the calculation.<sup>8</sup> Also note that (8) implies an effective bandwidth  $\sim 0.1U$ .

Finally, consider the case when  $\pi\Gamma \gg U$ , where the  $d$ -level width is so broad that the Anderson Hamiltonian may not be an adequate starting point. In this case one passes directly from the *free-orbital regime* (for  $k_B T > \Gamma$ ) to the *strong-coupling regime*. For  $k_B T \ll \Gamma$ ,  $\chi(T)$  is essentially temperature independent, and our calculations agree with the perturbation result

$$\chi(T) \approx \frac{(g\mu_B)^2}{2\pi\Gamma} \left[ 1 + \frac{U}{\pi\Gamma} + O\left(\frac{U}{\pi\Gamma}\right)^2 \right], \quad k_B T \ll \Gamma. \quad (9)$$

\*IBM Graduate Fellow.

†Research supported in part by the National Science Foundation under Grant No. MPS-74-19018.

‡Research supported in part by the National Science Foundation under Grant No. DMR-74-23494, 1975-1976 address: NORDITA, Blegdamsvej 17, DK-2100 Copenhagen, Denmark.

<sup>1</sup>P. W. Anderson, Phys. Rev. **124**, 41 (1961).

<sup>2</sup>K. G. Wilson, in *Nobel Symposia—Medicine and Natural Sciences*, edited by B. Lundqvist and S. Lund-

qvist (Academic, New York, 1973), Vol. 24, p. 68.

<sup>3</sup>K. G. Wilson, Rev. Mod. Phys. (to be published).

<sup>4</sup>Our calculational scheme is quite capable of handling the physically more relevant *asymmetric* case, when the orbital energy is not  $-U/2$  but an independent parameter  $\epsilon_d$ . We discuss the symmetric case here because it maps onto the Kondo Hamiltonian. The asymmetric case would map onto a Kondo problem *including potential scattering*.

<sup>5</sup>P. W. Anderson and A. M. Clogston, Bull. Am. Phys. Soc. **6**, 124 (1961), and unpublished; J. Kondo, Prog. Theor. Phys. **28**, 846 (1962); J. R. Schrieffer and P. A.

Wolff, Phys. Rev. **149**, 491 (1966).

<sup>6</sup>In Ref. 3 the Kondo susceptibility was given only for  $T < 6T_K$ . Consequently Fig. 1 is the first presentation of  $\chi(T)$  for an extensive temperature range. Numerical tabulation of the results are available from the authors.

<sup>7</sup>P. W. Anderson, Comments Solid State Phys. **5**, 73 (1973); K. K. Murata, thesis, Cornell University, 1971 (unpublished); G. Grüner and A. Zawadowski, Rep. Prog. Phys. **37**, 1497 (1974).

<sup>8</sup>A description of these techniques, as well as a more detailed account of the results, will be published elsewhere.

## Extremal Effects in Rotationally Inelastic Diffraction from Crystal Surfaces\*

R. Grant Rowe,† Lynn Rathbun, and Gert Ehrlich

Coordinated Science Laboratory,‡ Department of Metallurgy, and Department of Physics,  
University of Illinois at Urbana-Champaign, Urbana, Illinois 61801

(Received 21 May 1975)

Molecules diffracted from a crystal can exchange energy between translation and rotation. Such an interchange can lead to an extremum in the scattering angle as a function of the incident wavelength; this in turn concentrates scattered intensity at the extremal angle, causing a singularity in the differential cross section. Extremal scattering in rotationally inelastic collisions is explored quantitatively for the diffraction of hydrogenic molecules and shown to affect significantly experiments with thermal beams.

In the interaction of molecular gases with a crystal surface, the interchange of energy between translation and the internal degrees of freedom can have a profound effect on the coherent scattering. For hydrogen and its isotopes, the exchange of rotational with translational energy has just recently been observed in scattering from ionic crystals<sup>1,2</sup>: Strong new diffraction peaks are found, displaced from the elastic-scattering maxima. We wish to point out here that the intensity of these inelastic beams is governed by a new effect which causes singularities in the differential scattering cross section at certain critical angles.

Consider a beam of monoenergetic molecules, with wave vector  $\vec{k}_0$ , which on colliding with a crystal exchange rotational energy for energy of translational motion. The magnitude of the wave vector  $\vec{k}$  for the scattered molecules is related to  $\vec{k}_0$  by the requirement that the total energy be conserved, that is, by

$$k^2 - k_0^2 = 2m_g \Delta E(I)/\hbar^2. \quad (1)$$

Here  $\Delta E(I)$  is the energy transferred from rotation to translation in a molecule of mass  $m_g$ . The integer  $I$  labels the particular rotational transi-

tion involved.  $I=1$  denotes the transition in which the least amount of energy is lost from rotation and imparted to translation,  $I=2$  the next highest, and so on; negative integers label loss transitions, in which translational energy is given up to rotation. In diffraction from a surface, the component of momentum along the surface is also conserved, leading to

$$\vec{K} - \vec{K}_0 = 2\pi\vec{G}(mn). \quad (2)$$

$\vec{K}$  is the component of the wave vector in the plane of the scattering array, and  $\vec{G}(mn)$  is the vector to the point  $mn$  in the reciprocal lattice of the surface.

For the sake of simplicity, we restrict ourselves to molecules diffracted in the plane defined by the surface normal and the wave vector of the incident beam. Scattering is assumed to occur from a square array, with lattice constant  $a$ ; the projection of the incident beam upon this array is at  $45^\circ$  to the crystal axes, as indicated in Fig. 1. Under these special conditions elastic scattering is limited to channels with indices  $(mn)$ . The angle  $\theta$  between the scattered beam and the surface is now related to  $\theta_0$ , the angle between the incident beam and the surface,